

# The conserved salt bridge linking two C-terminal $\beta/\alpha$ units in homodimeric triosephosphate isomerase determines the folding rate of the monomer

César A. Reyes-López,<sup>1</sup> Edith González-Mondragón,<sup>2</sup> Claudia G. Benítez-Cardoza,<sup>1</sup> María E. Chánez-Cárdenas,<sup>3</sup> Nallely Cabrera,<sup>4</sup> Ruy Pérez-Montfort,<sup>4</sup> and Andrés Hernández-Arana<sup>2\*</sup>

<sup>1</sup>Laboratorio de Investigación Bioquímica, Postgrado Institucional en Biomedicina Molecular, ENMyH-Instituto Politécnico Nacional, D.F., México

<sup>2</sup>Departamento de Química, Área de Biofísicoquímica, Universidad Autónoma Metropolitana-Iztapalapa, D.F., México

<sup>3</sup>Laboratorio de Patología Vascul ar Cerebral, Instituto Nacional de Neurología y Neurocirugía Manuel Velasco Suárez, D.F., Mexico

<sup>4</sup>Departamento de Bioquímica, Instituto de Fisiología Celular, Universidad Nacional Autónoma de México, D.F., México

## ABSTRACT

Triosephosphate isomerase (TIM), whose structure is archetypal of dimeric  $(\beta/\alpha)_8$  barrels, has a conserved salt bridge (Arg189–Asp225 in yeast TIM) that connects the two C-terminal  $\beta/\alpha$  segments to rest of the monomer. We constructed the mutant D225Q, and studied its catalysis and stability in comparison with those of the wild-type enzyme. Replacement of Asp225 by Gln caused minor drops in  $k_{cat}$  and  $K_M$ , but the catalytic efficiency ( $k_{cat}/K_M$ ) was practically unaffected. Temperature-induced unfolding–refolding of both TIM samples displayed hysteresis cycles, indicative of processes far from equilibrium. Kinetic studies showed that the rate constant for unfolding was about three-fold larger in the mutant than in wild-type TIM. However, more drastic changes were found in the kinetics of refolding: upon mutation, the rate-limiting step changed from a second-order (at sub-micromolar concentrations) to a first-order reaction. These results thus indicate that renaturation of  $\gamma$ TIM occurs through a uni-bimolecular mechanism in which refolding of the monomer most likely begins at the C-terminal half of its polypeptide chain. From the temperature dependence of the refolding rate, we determined the change in heat capacity for the formation of the transition state from unfolded monomers. The value for the D225Q mutant, which is about 40% of the corresponding value for  $\gamma$ TIM, would implicate the folding of only three quarters of a monomer chain in the transition state.

Proteins 2008; 72:972–979.  
© 2008 Wiley-Liss, Inc.

**Key words:** dimeric TIM barrel; thermal unfolding/refolding profiles; refolding kinetics; salt bridge; transition state.

## INTRODUCTION

Parallel folding channels and partially folded intermediates seem to be commonplace in folding reactions of proteins of moderate to large size. For instance, the refolding of the  $\alpha$ -subunit of tryptophan synthase ( $\alpha$ TS), a monomeric, single-domain,  $(\beta/\alpha)_8$ -barrel protein, displays multiple kinetic phases spanning a large time scale.<sup>1</sup> Mathews and coworkers<sup>1–3</sup> proposed that the refolding mechanism of  $\alpha$ TS involves both off- and on-pathway intermediates, as well as the occurrence of at least four parallel reaction channels. Most likely, some of these intermediates are partially folded forms, identified in previous equilibrium and kinetic studies<sup>4,5</sup> as autonomous folding units, each comprising a particular region of the polypeptide chain. Formation of the most stable intermediate apparently corresponds to the folding of the first six  $\beta/\alpha$  modules (i.e., residues 1–188); after this event, the remaining two  $\beta/\alpha$  units fold and assemble to the rest of the protein<sup>2,4</sup>; accordingly,  $\alpha$ TS is said to follow a 6 + 2 folding model. This proposal notwithstanding, reports on the stability of amino-terminal fragments of  $\alpha$ TS<sup>6,7</sup> indicate a different, 4 + 2 + 2 folding model. In this regard, the presence of both on- and off-pathway intermediates and of several folding channels in  $\alpha$ TS may be a reflection of the many ways in which discrete  $\beta\alpha\beta$  modules can associate to form native-like or nonnative-like structures.<sup>2</sup> Currently, there is also some lack of agreement regarding the folding mechanism

The Supplementary Material referred to in this article can be found online at <http://www.interscience.wiley.com/jpages/0887-3585/suppmat/>

Grant sponsor: CONACyT, México; Grant number: SEP-2003-CO2-44681.

\*Correspondence to: Andrés Hernández Arana, Área de Biofísicoquímica, Departamento de Química, Universidad Autónoma Metropolitana-Iztapalapa, Apartado Postal 55-534, Iztapalapa, D.F., 09340, México. E-mail: [aha@xanum.uam.mx](mailto:aha@xanum.uam.mx)

Received 1 October 2007; Revised 3 December 2007; Accepted 28 December 2007

Published online 25 February 2008 in Wiley InterScience (www.interscience.wiley.com).

DOI: 10.1002/prot.21994

of N-(5'-phosphoribosyl) anthranilate isomerase (PRAI), another monomeric ( $\beta/\alpha$ )-barrel protein.<sup>8–12</sup> It is clear, however, that the most stable region of, and also the first to be folded in, both  $\alpha$ TS and PRAI includes four to six  $\alpha/\beta$  modules, starting from the N-terminus of the chain.

The folding of dimeric ( $\beta/\alpha$ )-barrel molecules has not been so extensively studied. However, recent results about the temporal order on which different regions of the barrel fold are in contrast with those mentioned above for  $\alpha$ TS and PRAI. Indeed, by means of amide exchange and mass spectrometry, Pan *et al.*<sup>13</sup> have shown that the monomer of rabbit muscle triosephosphate isomerase (rabbit TIM) may be divided into halves: a fast folding domain, comprising the four C-terminal  $\beta/\alpha$  units, and a slow folding domain, which is formed by the remaining N-terminal modules. Furthermore, folding of the C-terminal half apparently leads to a partially folded monomer of marginal stability, which can be detected as a kinetic intermediate in low concentration of guanidine hydrochloride (GuHCl).<sup>13</sup> It should be mentioned, however, that monomeric, partially folded conformations of yeast (*Saccharomyces cerevisiae*) TIM have been found to be well populated states at equilibrium in about 1.0M GuHCl.<sup>14,15</sup> In particular, Silverman and Harbury<sup>16</sup> used the method of misincorporation proton-alkyl exchange to determine the apparent stabilities of three subdomains of the yeast TIM monomer; their results indicate that unfolding proceeds along a sequential model, with two intermediate states, in which the first three N-terminal  $\beta/\alpha$  units comprise the most stable subdomain. Interestingly, bioinformatical approaches<sup>17,18</sup> have revealed two important folding-initiation sites in the family of TIM proteins. One of them resides precisely in a DX(D/N)G motif located just before  $\beta$ -strand 8. In all TIM structures, the conserved Asp residue in this motif forms a salt bridge with a basic residue in helix 6.<sup>19,20</sup> The relevance of this salt bridge may be found in the fact that it acts (together with other residues forming a network of hydrogen bonds) as a link that anchors the C-terminal ( $\beta/\alpha$ )<sub>7–8</sub> segment to the rest of the protein.<sup>20,21</sup> Indeed, as reported by Kursula *et al.*,<sup>21</sup> disruption of the aforementioned interaction (i.e., Arg191–Asp227 in *Trypanosoma brucei* TIM) by substitution of either of both charged partners leads to mutant enzymes with good catalytic activity, but whose refolding efficiency (after being unfolded in GuHCl) was drastically abolished in comparison with the wild-type enzyme.

Since it is not known how the disruption of the conserved salt bridge affects the stability and refolding kinetics of TIM, in this work we have investigated these matters in a point mutant of *Saccharomyces cerevisiae* TIM ( $\gamma$ TIM), in which Asp225 (equivalent to Asp227 in trypanosome TIM) was substituted by Gln. As has been shown previously,<sup>22</sup> when present in submicromolar concentrations thermally unfolded  $\gamma$ TIM recovers its secondary structure through a second-order reaction charac-

terized by a compact, main transition state (TS). In contrast, here we report that refolding of the D225Q mutant follows first-order kinetics and the main TS seems to bury much less surface area. On the other hand, the mutation of Asp225 only barely affected the unfolding reaction and the catalytic efficiency of the enzyme.

## MATERIALS AND METHODS

### Mutagenesis and protein expression and purification

The change of the Asp225 for Gln was performed by polymerase chain reaction (PCR)-based overlap extension mutagenesis.<sup>23</sup> Mutagenic oligonucleotides were as follows: 5'-AAGGACAAGGCTCAGGTCGATGGTTTC-3' for the forward extension, and 5'-GAATCCATCGACCTGAGCCTTGTCCTT-3' for the reverse. Promoter and terminator T7 oligonucleotides were used to complete the amplification of the gene. The mutant gene was cloned in the pET3a vector (pET System, Novagen). After verifying the mutagenic codon incorporation by gene complete sequence, the plasmid was used to transform BL21(DE3)-pLysS cells.

Overexpression and purification of the wild-type and D225Q TIM were carried out as described by Vázquez-Contreras *et al.*<sup>24</sup> Anion-exchange FPLC and SDS-PAGE analysis showed that TIM preparations were homogeneous. Protein concentration was determined using the absorption coefficient at 280 nm,  $A_{1\text{ cm}}^{1\%} = 10.0$ .<sup>25</sup>

### Activity assays

Enzyme activity was determined by a coupled assay with  $\alpha$ -glycerophosphate dehydrogenase ( $\alpha$ -GDH) in the direction of D-glyceraldehyde 3-phosphate (DGAP) to dihydroxyacetone phosphate (DHAP), following NADH oxidation by absorbance changes at 340 nm.<sup>26</sup> Routinely, assays were made at 25.0°C in a 1.0-mL mixture containing buffer A [100 mM triethanolamine (TEA), 10 mM EDTA, pH 7.4], 0.20 mM NADH, 0.02 mg of  $\alpha$ -GDH, and 2.0 mM DGAP. The reaction was initiated by the addition of 3.0 ng of TIM. For the determination of  $K_m$  and  $k_{\text{cat}}$ , the concentration of DGAP was varied between 0.05 and 4.0 mM.

### Spectroscopic methods

Fluorescence spectra were obtained at 25.0°C in a PC1 spectrofluorometer (ISS, Champaign, IL). TIM samples (0.050 mg mL<sup>-1</sup>) were excited at 280 nm, and emission was collected from 300 to 400 nm. Circular dichroism (CD) studies were carried out using a J-715 spectropolarimeter (JASCO, Easton, MD) equipped with a PTC-348WI Peltier-type cell holder for temperature control and magnetic stirring. Protein solutions of about 0.10 mg mL<sup>-1</sup> were placed in a 0.10-cm quartz cell for

recording of spectra (250–190 nm). For thermal scans and kinetic experiments, we employed 1.00-cm cells where protein concentration can be lowered to  $\sim 10 \mu\text{g mL}^{-1}$ , thus reducing the risk of protein aggregation after thermal denaturation. Temperature-induced unfolding transitions were followed by continuous monitoring of the ellipticity at 220 nm while the sample was heated at a rate of  $3.0^\circ\text{C min}^{-1}$ ; the actual temperature of the protein solution was measured with the external immersion probe of the Peltier accessory. After unfolding had been completed, the sample was cooled at the same rate to register the refolding profile.

Tracings of the kinetics of unfolding and refolding were obtained by following ellipticity changes at 220 nm, as described before.<sup>22</sup> Unfolding was initiated by adding a small aliquot of concentrated TIM solution to a cell containing buffer equilibrated at a desired temperature. In refolding experiments, TIM samples were first subjected to a temperature high enough to induce unfolding of the protein in  $\sim 1.5$  min. Then, the temperature control of the Peltier accessory was set to a value  $4.0^\circ\text{C}$  below the temperature intended for the study of the refolding reaction, thus allowing for a fast cooling ( $\sim 15^\circ\text{C min}^{-1}$ ) of the sample; the final temperature value was entered into the cell-holder control when the cell was  $0.5^\circ\text{C}$  above the desired value, and the CD signal was registered thereafter. Inside the cell, temperature came to equilibrium ( $\pm 0.15^\circ\text{C}$ ) in  $\sim 40$  s. An alternative procedure was also used to study refolding of the wild-type enzyme, which has proven to be more resistant to irreversible aggregation than its mutants.<sup>22,27</sup> In this case, a concentrated protein sample ( $100 \mu\text{g mL}^{-1}$ ) was unfolded at high temperature, as mentioned above; 200–300  $\mu\text{L}$  of this solution was added to 2.700–2.800 mL of buffer previously equilibrated to the temperature of the study. Thermal equilibration of the final solution took about 25 s.

## RESULTS AND DISCUSSION

### Expression, catalytic, and structural properties of the D225Q mutant

Production of the mutant enzyme from transformed *Escherichia coli* cells was about 3.0 mg per liter of culture, which is four times less than the amount of wild-type enzyme obtained from similar cultures. As SDS-PAGE indicated, lower yields of the mutant are apparently due to lower expression levels, and not to aggregation of the expressed protein (Fig. S1 in Supplementary Material).

CD and fluorescence spectra (recorded at  $25.0^\circ\text{C}$ ) of purified D225Q TIM display no significant differences with respect to those of  $\gamma\text{TIM}$  (Figs. S2 and S3 in Supplementary Material). Similarly, the catalytic properties of the enzyme changed only slightly upon mutation of Asp 225 (Table I). As can be seen, minor drops in  $k_{\text{cat}}$  and  $K_{\text{M}}$  com-

**Table I**  
Catalytic Properties of  $\gamma\text{TIM}$  and its D225Q Mutant<sup>a</sup>

	$k_{\text{cat}} \times 10^{-3} (\text{s}^{-1})$	$K_{\text{M}} (\text{mM})$	$k_{\text{cat}}/K_{\text{M}} \times 10^{-6} (\text{s M})^{-1}$
$\gamma\text{TIM}$	6.9 (0.4)	1.13 (0.2)	6.1
D225Q	4.6 (0.04)	0.91 (0.08)	5.0

<sup>a</sup> $k_{\text{cat}}$  and  $K_{\text{M}}$  were determined from activity assays carried out at  $25^\circ\text{C}$ , pH 7.4, with D-glyceraldehyde 3-phosphate as substrate.

pensate each other so that the catalytic efficiency ( $k_{\text{cat}}/K_{\text{M}}$ ) of the enzyme is unaffected by this mutation.

### Thermal scans

Melting-transition profiles of wild-type and D225Q TIM were first obtained by temperature scanning ( $3.0^\circ\text{C}/\text{min}$ ) of samples dissolved in 0.01M Tris buffer, pH 7.4. The apparent  $T_{\text{m}}$  for the mutant was  $\sim 3.0^\circ\text{C}$  below that for the wild-type enzyme. In this regard, it should be mentioned that the method iPREE-STAB<sup>28</sup> predicts this particular mutation as slightly structure destabilizing. When the wild-type protein was cooled to  $25^\circ\text{C}$ , after being thermally unfolded, more than 80% of the molecules were able to refold, giving rise to the hysteresis unfolding–refolding cycle that has been reported previously.<sup>22,27</sup> The thermally unfolded mutant, however, showed only about 20% refolding upon cooling. Poor refolding capacity (i.e., ca. 2% recovery of enzymatic activity) has also been found in *Trypanosoma brucei brucei* TIM variants in which the conserved salt bridge had been broken by point mutations.<sup>21</sup>

Nevertheless, we found that the refolding efficiency of D225Q  $\gamma\text{TIM}$  notably improved in the presence of phosphate ions. Figure 1 shows unfolding–refolding cycles for the two enzymes under study, recorded with samples prepared in 0.01M phosphate buffer, pH 7.4. In this buffer, the mutant enzyme showed better refolding (i.e., ca. 60%), as judged from its CD spectrum and the recovery of enzyme activity after refolding. Besides,  $T_{\text{m}}$  values were  $\sim 2^\circ\text{C}$  higher in phosphate than in Tris buffer, indicating that phosphate ions, which are weak inhibitors of TIM enzymes,<sup>29</sup> exert stabilizing effects on both proteins. It is important to note that CD spectra of thermally unfolded TIM variants recorded at  $68^\circ\text{C}$  (Fig. S4 in Supplementary Material) indicated that the loss of secondary structure in unfolded TIMs is essentially the same either in Tris or phosphate buffer. Thus, although the phosphate ion does not significantly affect the residual structure of thermally unfolded  $\gamma\text{TIM}$ , its presence seems to help unfolded molecules to avoid side reactions that lead to irreversible aggregation. Weak, specific or nonspecific, binding of phosphate ions to the unfolded molecule might be causing a reduction of solvent-exposed “sticky” surfaces, which are prone to form aggregates.

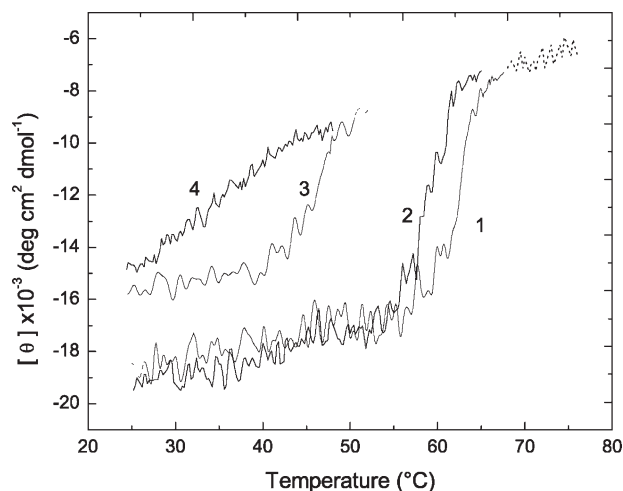


**Figure 1**

Temperature-induced unfolding and refolding profiles of wild-type yeast TIM and its D225Q mutant. Transitions were registered by continuous monitoring of the ellipticity at 220 nm, with heating or cooling rates of  $3.0^{\circ}\text{C min}^{-1}$ . Protein solutions of  $10\ \mu\text{g mL}^{-1}$ , in  $0.01\text{M}$  phosphate buffer (pH 7.4), and  $1.00\text{-cm}$  cuvettes were used. Curves 1 and 2 correspond to the heating of the wild-type enzyme and the mutant, respectively. When unfolding had been completed, samples were quickly cooled to  $53\text{--}52^{\circ}\text{C}$  and recording of the refolding transition (curve 3,  $\gamma\text{TIM}$ ; curve 4, D225Q mutant) was then started. The dashed line extending from  $68$  to  $75^{\circ}\text{C}$  shows the posttransition CD signal, which was registered in separate experiments.

It is also noted in Figure 1 that substitution of Asp225 for Gln brings about a larger shift in the apparent  $T_m$  corresponding to, and also some broadening of, the refolding arm of the hysteresis curve. Because under the experimental conditions imposed the overall unfolding–refolding process is kinetically controlled, one should expect the mutation to cause larger alterations on the refolding kinetics of the protein.

### Unfolding kinetics

Temperature-induced unfolding of wild-type  $\gamma\text{TIM}$  was studied in the  $56\text{--}65^{\circ}\text{C}$  range, in  $0.01\text{M}$  phosphate buffer, pH 7.4. Results (Fig. S5 in Supplementary Material) indicated that phosphate ions do not change the general characteristics of the unfolding reaction that were found before<sup>22</sup>; that is, the reaction follows simple first-order kinetics and leads to complete unfolding (as judged by the CD signal) at all temperatures studied. At  $65.0^{\circ}\text{C}$ , unfolding was completed in  $\approx 1.5$  min; rapid cooling of the sample to temperatures below  $50^{\circ}\text{C}$  allowed the enzyme to refold  $\sim 90\%$ , and also to recover its catalytic activity in a similar percentage. However, as the unfolding process took longer time, the enzyme lost its ability to refold and recover catalytic activity upon cooling. As discussed before,<sup>22,27</sup> these characteristics of TIM

unfolding point out not only the absence of equilibrium between native dimer and unfolded monomers, but also the occurrence of further reactions that lead to irreversibly unfolded species (i.e., aggregates).

Unfolding studies carried out with the mutant gave similar results, except that maximal refolding was somewhat smaller (ca. 85%) than in the case of the wild-type enzyme. Besides, the mutant proved to be kinetically less stable than  $\gamma\text{TIM}$ ; that is, the unfolding rate constant,  $k_u$ , for the mutant was approximately three times larger than that for the wild-type enzyme, as can be seen in the Eyring plots of Figure 2. These plots show that  $k_u$  behaves according to Eyring's equation:

$$\ln(k_u/T) = \ln(k_B/h) + \Delta S^{\ddagger}/R - (\Delta H^{\ddagger}/R)(1/T) \quad (1)$$

for the particular case in which the activation enthalpy ( $\Delta H^{\ddagger}$ ) and entropy ( $\Delta S^{\ddagger}$ ) are both independent of temperature;  $k_B$  and  $h$  stand for Boltzmann's and Planck's constants, respectively. From least-squares fits of Eq. (1) to the experimental data,  $\Delta H^{\ddagger}$  was calculated as 495 and  $400\ \text{kJ mol}^{-1}$  for the wild-type and the D225Q enzymes, respectively. Results obtained from these fittings are summarized in Table II.

### Refolding kinetics

It has been found<sup>22,27</sup> that refolding of  $\gamma\text{TIM}$  follows second order kinetics when studied in Tris buffer (pH

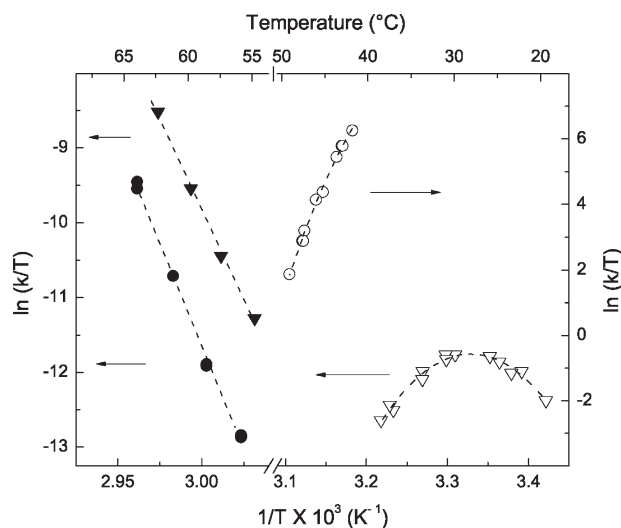


**Figure 2**

Eyring plots for the unfolding ( $k_u$ ) and refolding ( $k_r$ ) rate constants of  $\gamma\text{TIM}$  and its D225Q mutant. Rate constants were determined from far-UV CD kinetic experiments carried out in  $0.01\text{M}$  phosphate buffer, pH 7.4. Data for  $\gamma\text{TIM}$  are shown with filled (unfolding) and open (refolding) circles. Filled and open triangles indicate unfolding and refolding data for the D225Q mutant, respectively. Lines shown correspond to least-squares regressions to Eq. (1) (unfolding) or Eq. (2) (refolding).

**Table II**Unfolding and Refolding Activation Parameters of  $\gamma$ TIM and its D225Q Mutant<sup>a</sup>

	Unfolding				Refolding			
	$\Delta H^\ddagger$	$\Delta S^\ddagger$	$\Delta G^\ddagger$	$\Delta C_p^\ddagger$	$\Delta H^\ddagger$	$\Delta S^\ddagger$	$\Delta G^\ddagger$	$\Delta C_p^\ddagger$
$\gamma$ TIM	495 (14)	1190 (43)	126 (2)	0	-230 (47)	-873 (160)	41 (12)	-32 (6)
D225Q	400 (15)	920 (46)	115 (1)	0	-129 (7)	-712 (20)	92 (3)	-13.4 (0.7)

<sup>a</sup> $\Delta C_p^\ddagger$ , as well as  $\Delta H^\ddagger$  and  $\Delta S^\ddagger$  for unfolding, are temperature independent parameters. All other values are given at 37°C.  $\Delta H^\ddagger$  and  $\Delta G^\ddagger$  are in kJ mol<sup>-1</sup>,  $\Delta C_p^\ddagger$  is in kJ/(mol K), and  $\Delta S^\ddagger$  is in J/(mol K). Standard deviation is shown in parentheses below each value.

8.4), at submicromolar concentration. Because in the present work we used phosphate buffer (pH 7.4), we first checked whether the presence of phosphate ions alters or not the known features of the reaction. According to procedures described in Materials and Methods, the time course of  $\gamma$ TIM refolding was studied in the range from 41 to 49°C. The kinetics of this process (see Fig. 3) was found to differ from previous results in two aspects. First, about 15–20% of the protein ellipticity was recovered within the dead time of experiments; in studies carried out in Tris buffer (pH 8.5) no significant fast-folding phase had been observed. Second, the major slow phase, which was the one actually registered, followed second-order kinetics only when protein concentration was less than 20  $\mu\text{g mL}^{-1}$  (i.e., 0.75  $\mu\text{M}$  TIM monomers), as indicated by the dependence of the reaction half-time ( $t_{1/2}$ ) on the protein concentration (see Fig. 4). For a second-order reaction,  $t_{1/2}$  is related to the total concentration of reactant,  $C_0$ , by  $t_{1/2} = 1/2C_0k_r$ , where  $k_r$  is the rate constant. However, it is seen in Figure 4 that at concentrations above 20  $\mu\text{g mL}^{-1}$   $t_{1/2}$  slightly deviates from the expected trend, suggesting that the limiting step for the reaction is changing from second to first order.

Refolding of the D225Q mutant was also studied in phosphate buffer (pH 7.4), but at temperatures varying from 19 to 38°C. The kinetics resembled the behavior of wild-type TIM in that a fast phase of small amplitude was observed (see Fig. 3); nevertheless, the reaction half-time for the second, slow phase was in this case nearly independent of protein concentration as in a first-order reaction (see Fig. 4). Such a change in the molecularity of the rate-limiting folding step suggests that the TIM molecule refolds through a sequential uni-bimolecular pathway in which an unstable, monomeric intermediate appears before the association step. Formation of secondary structure in the intermediate would involve, at least, helix 6 and the two C-terminal  $\beta/\alpha$  units, which are regions linked together by the salt bridge Asp225–Arg189. Weakening or disruption of this interaction would then increase the folding barrier for the unimolecular step, thus making it rate limiting, as observed with the mutant D225Q. Furthermore, the refolding rate-enhancing effect of phosphate seems to indicate that the intermediate is stabilized by this ion. If so, the region

structured in the first step may extend to the loop connecting  $\beta$ -strand 6 to helix 6, in as much as this loop comprises some residues that interact with the phosphate group of the substrate.<sup>30</sup> We must remind, however, that a small amount of secondary structure might remain in thermally unfolded TIM.<sup>22</sup> Nevertheless, such a residual structure should be very limited in extent and stability, as judged from the calorimetric enthalpy of TIM unfolding which, when normalized on a per residue basis, results in a value close to that observed for small proteins regarded as completely unfolded from a thermodynamic point of view (see Refs. 22 and 31). It is possible indeed that parts of the C-terminal  $\beta$  strands persist as flickering structures at high temperature, but they consolidate into native  $\beta/\alpha$  modules by interaction with their adjacent  $\alpha$ -helical regions at temperatures where the native protein is stable.

Results presented above suggest, therefore, that parts of the C-terminal half of  $\gamma$ TIM conform a structural nucleus that is folded in an initial stage of the folding pathway of this protein, in agreement with the idea that Pan *et al.*<sup>13</sup> proposed based on their studies with rabbit muscle TIM. In contrast, the apparent stabilities of  $\gamma$ TIM subdomains that were determined by Silverman and Harbury<sup>16</sup> might lead one to think that the three N-terminal  $\beta/\alpha$  units, which are the most stable region in equilibrium GuHCl-induced unfolding experiments, represent the site of initial structure formation on the monomer folding pathway. However, as these authors recognize,<sup>16</sup> “knowledge of the equilibrium unfolding pathway cannot, in itself, determine the kinetic folding pathway.” Indeed, a partially folded intermediate state that is stable at some denaturant concentration may not be populated at all when the protein refolds in the absence of denaturant.

It may be thought, on the other hand, that the fast kinetic phase detected in our CD studies could be a reflection of an early development of secondary structure in the polypeptide chain that occurs even before the structural consolidation of the C-terminal  $\beta/\alpha$  modules. To elucidate this point, we studied the recovery of enzyme activity during renaturation. For both,  $\gamma$ TIM and D225Q, a minor amount of activity (i.e., ca. 15% in the wild-type enzyme and 20% in the mutant) was recovered

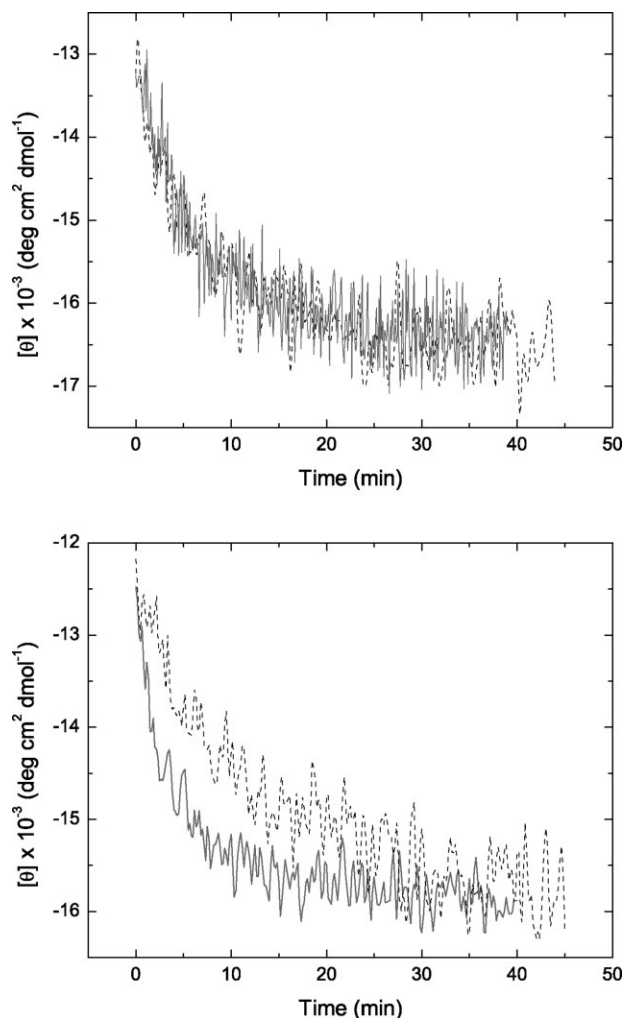


**Figure 3**

Effect of protein concentration on the refolding kinetics of the D225Q mutant (A) and wild-type TIM (B). Refolding was followed by the change in ellipticity at 220 nm, in a 1.00-cm cell. In panel A, kinetic tracings correspond to protein concentrations of 10 (dotted line) and 30 μg mL<sup>-1</sup> (solid line in gray), both registered at 30.0°C. Curves shown in panel B were recorded at 49.0°C with protein concentrations of 7.5 (dotted line) and 20 μg mL<sup>-1</sup> (gray line).

within the dead time of kinetic experiments (see Fig. 5). The remaining regain of activity took place with a half time only slightly longer than that observed for the major, slow-refolding phase. Therefore, the fast kinetic phase is most likely due to the coexistence of fast-folding ( $U_F$ ) and slow-folding ( $U_S$ ) unfolded states which can both refold through parallel pathways leading to the fully renatured enzyme, rather than to the formation of an early, rudimentarily folded intermediate. In this regard, it is frequently found that the slow interconversion between  $U_S$  and  $U_F$  species is associated to prolyl peptide bond isomerization; in general, however, a high fraction of  $U_S$  is expected only when the native state has one or more

*cis* prolyl bonds,<sup>32</sup> which is not the case of  $\gamma$ TIM whose five proline residues are all in *trans* conformation. Furthermore, since the amplitude of the fast renaturation reaction of  $\gamma$ TIM and its mutant seems to depend on the presence of phosphate groups, the occurrence of a significant fraction of  $U_F$  species might be attributed to a conformational change linking unfolded forms with different affinity for this ligand. Respecting this matter, the discrepancy between our proposal for the refolding pathway of  $\gamma$ TIM and that inferred from the results of Silverman and Harbury<sup>16</sup> may be due to the presence of phosphate ions in our studies. In any case, since phosphate is a ubiquitous component of living organisms, its presence must be taken into account in any model that looks for an understanding of how proteins fold *in vivo*.

### Temperature dependence of refolding rate-constants

Figure 2 shows the variation of  $k_r$  with temperature, in the form of Eyring's plots for  $\gamma$ TIM and its mutant. Data were analyzed by using Eq. (2),<sup>22</sup>

$$\ln(k_r/T) = A - B(1/T) - (\Delta C_p^\ddagger/R) \ln(1/T) \quad (2)$$

where  $\Delta C_p^\ddagger$  represents the change in heat capacity upon formation of the refolding TS. Coefficient  $B$  can be

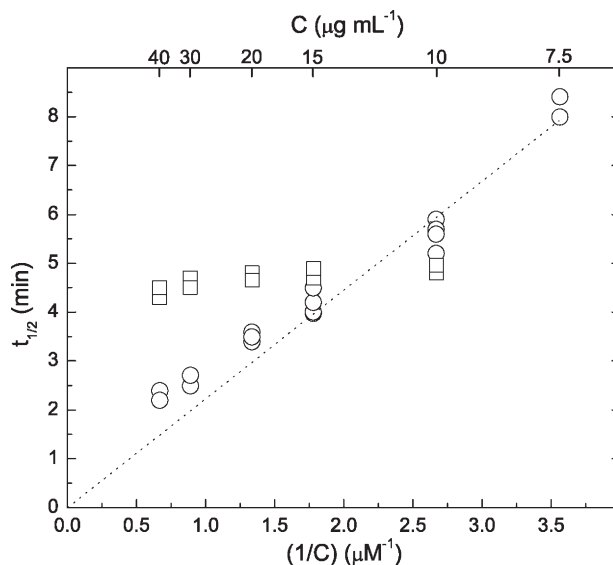


**Figure 4**

Dependence of the half-life time ( $t_{1/2}$ ) of the refolding reaction on protein concentration. Data for wild-type TIM (circles) were obtained from kinetic experiments carried out at 49.0°C; for the D225Q mutant (squares), data correspond to 30.0°C. The bottom X axis indicates the reciprocal of monomer micromolarity, which was calculated with  $M_r = 26,650$ , whereas protein concentration in μg mL<sup>-1</sup> is shown on the top axis. The line is the expected trend for a second-order reaction.

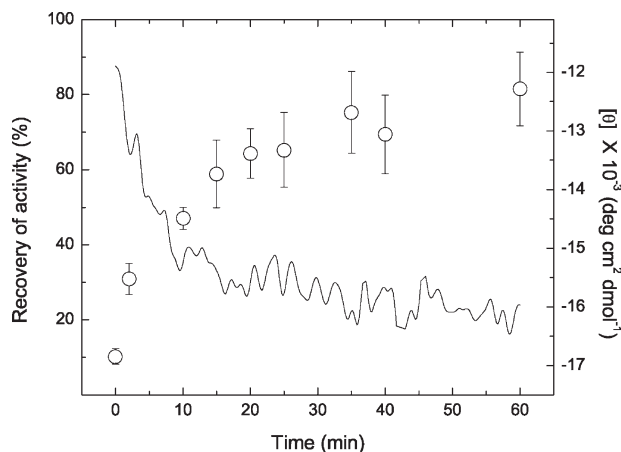


**Figure 5**

Time course of wild-type TIM refolding (49.0°C) as followed by CD (solid line) and the recovery of enzymatic activity (circles). In both experiments protein concentration is 10  $\mu\text{g mL}^{-1}$ . CD data were registered as in Figure 3.

expressed as a combination of activation “thermodynamic” functions as follows:  $B = (\Delta H_r^\ddagger - \Delta C_p^\ddagger T_R)/R$ , from which the enthalpy of activation,  $\Delta H_r^\ddagger$ , can be calculated at any particular temperature,  $T_R$ , chosen as reference. The temperature-independent term,  $A$ , is given by:  $A = \ln(k_B/h) + (\Delta S_r^\ddagger - \Delta C_p^\ddagger - \Delta C_p^\ddagger \ln T_R)/R$ . Fitting of Eq. (2) to refolding data yielded negative values of  $\Delta C_p^\ddagger$ , in accord with the downward curvature of plots shown in Figure 2. For wild-type TIM,  $\Delta C_p^\ddagger$  was determined as  $32 \pm 6 \text{ kJ}/(\text{K mol})$ , which is identical to the value found at pH 8.5<sup>22</sup>; in comparison, the value of  $\Delta C_p^\ddagger$  found for refolding of D225Q TIM was only  $13.4 \pm 0.8 \text{ kJ}/(\text{K mol})$ . Because it is thought that heat capacity changes taking place in protein structural transitions are roughly proportional to the respective changes in solvent-accessible surface area, the aforementioned values of  $\Delta C_p^\ddagger$  indicate that the TS for the mutant buries only  $\approx 40\%$  of the area buried in the TS of wild-type TIM. Further characterization of TS can be obtained by means of a well-known parameterization relating thermodynamic functions to polar and apolar surface areas that become buried on protein folding.<sup>31</sup> The equations pertinent to the analysis of refolding kinetics are written as:

$$\Delta H_r^\ddagger = \Delta H^* \Delta \text{ASA}_{\text{pol}}^\ddagger + \Delta C_p^\ddagger (T - T_H) \quad (3)$$

$$\Delta C_p^\ddagger = \Delta C_{p, \text{pol}} \Delta \text{ASA}_{\text{pol}}^\ddagger + \Delta C_{p, \text{ap}} \Delta \text{ASA}_{\text{ap}}^\ddagger \quad (4)$$

wherefrom changes in polar ( $\Delta \text{ASA}_{\text{pol}}^\ddagger$ ) and apolar ( $\Delta \text{ASA}_{\text{ap}}^\ddagger$ ) solvent-accessible surface area occurring when TS is formed can be computed from experimentally determined values of  $\Delta C_p^\ddagger$  and  $\Delta H_r^\ddagger$ ; other terms appear

in Eqs. (3) and (4) represent parameters of general validity whose values are<sup>31</sup>:  $\Delta H^* = 35 \text{ cal} (\text{mol } \text{Å}^2)^{-1}$ ;  $T_H = 373 \text{ K}$ ;  $\Delta C_{p, \text{pol}} = -0.26 \text{ cal K}^{-1} (\text{mol } \text{Å}^2)^{-1}$ ;  $\Delta C_{p, \text{ap}} = 0.45 \text{ cal K}^{-1} (\text{mol } \text{Å}^2)^{-1}$ . By introducing data for the mutant D225Q into the aforementioned equations, we found that the main TS on the folding pathway buries  $6400 \text{ Å}^2$  of polar and  $10,800 \text{ Å}^2$  of apolar area, adding up to a total of  $17,200 \text{ Å}^2$ . Since the total area buried in folded proteins amounts on an average to  $90\text{--}100 \text{ Å}^2$  per residue,<sup>31</sup> the total area buried when TS is formed would be equivalent to the folding of about 180 residues (i.e., three-quarters of the 248-residue-long chain of a TIM monomer). In the case of wild-type TIM, similar calculations gave a total buried area in TS of  $41,200 \text{ Å}^2$  ( $15,300$  and  $25,900 \text{ Å}^2$  of polar and apolar areas, respectively); this quantity would be compatible with the folding of about 430 residues, thus conveying the notion of a dimeric TS with native-like conformation.

## CONCLUDING REMARKS

To disrupt the conserved Arg189–Asp225 salt bridge in yeast TIM, the aspartic residue was replaced by glutamine. This mutation only barely affected the catalytic activity of the enzyme, but otherwise largely reduced the enzyme’s refolding rate. Furthermore, the D225Q mutation changed the kinetics of the rate-limiting step in refolding from second to first order; concomitantly, the magnitude of the (negative) heat capacity change associated to the formation of the TS decreased more than two-fold in the mutant. These results indicate that renaturation of the TIM dimer starts with the refolding of, at least, three of the C-terminal  $\beta/\alpha$  units, which are linked together by the conserved salt bridge; hindering of this interaction, as in D225Q TIM, causes the first folding step to become rate limiting. The monomeric intermediate resulting from the above reaction seems to be largely structured, but unstable under physiological conditions. The ensuing bimolecular association step is fast and becomes rate limiting (in wild-type TIM) only at sub-micromolar concentrations.

## REFERENCES

1. Bilsel O, Zitzewitz JA, Bowers KE, Matthews CR. Folding mechanism of the  $\alpha$ -subunit of tryptophan synthase, an  $\alpha/\beta$  barrel protein: global analysis highlights the interconversion of multiple native, intermediate, and unfolded forms through parallel channels. *Biochemistry* 1999;38:1018–1029.
2. Zitzewitz JA, Matthews CR. Molecular dissection of the folding mechanism of the  $\alpha$  subunit of tryptophan synthase: an amino-terminal autonomous folding unit controls several rate-limiting steps in the folding of a single domain protein. *Biochemistry* 1999;38:10205–10214.
3. Wintrode PL, Rojsajakul T, Vadrevu R, Matthews CR, Smith DL. An obligatory intermediate controls the folding of the  $\alpha$ -subunit of tryptophan synthase: a TIM barrel protein. *J Mol Biol* 2005;347:911–919.

4. Miles EW, Yutani K, Ogasahara K. Guanidine hydrochloride induced unfolding of the  $\alpha$  subunit of tryptophan synthase and of the two  $\alpha$  proteolytic fragments: evidence for stepwise unfolding of the two  $\alpha$  domains. *Biochemistry* 1982;21:2586–2592.
5. Higgins W, Fairwell T, Miles EW. An active proteolytic derivative of the alpha subunit of tryptophan synthase. Identification of the site of cleavage and characterization of the fragments. *Biochemistry* 1979;18:4827–4835.
6. Zitzewitz JA, Gualfetti PJ, Perkons IA, Wasta SA, Matthews CR. Identifying the structural boundaries of independent folding domains in the alpha subunit of tryptophan synthase, a  $\beta/\alpha$  barrel protein. *Protein Sci* 1999;8:1200–1209.
7. Rojsajjakul T, Wintrode P, Vadrevu R, Matthews CR, Smith DL. Multi-state unfolding of the alpha subunit of tryptophan synthase, a TIM barrel protein: insights into the secondary structure of the stable equilibrium intermediates by hydrogen exchange mass spectrometry. *J Mol Biol* 2004;341:241–253.
8. Luger K, Hommel U, Herold M, Hofsteenge J, Kirschner K. Correct folding of circularly permuted variants of a  $\beta\alpha$  barrel enzyme *in vivo*. *Science* 1989;243:206–210.
9. Jasanoff A, Davis B, Fersht AR. Detection of an intermediate in the folding of the  $(\beta\alpha)_8$ -barrel N-(5'-phosphoribosyl)anthranilate isomerase from *Escherichia coli*. *Biochemistry* 1994;33:6350–6355.
10. Akanuma S, Yamagishi A. Identification and characterization of key substructures involved in the early folding events of a  $(\beta/\alpha)_8$ -barrel protein as studied by experimental and computational methods. *J Mol Biol* 2005;353:1161–1170.
11. Akanuma S, Miyagawa H, Kitamura K, Yamagishi A. A detailed unfolding pathway of a  $(\beta/\alpha)_8$ -barrel protein as studied by molecular dynamics simulations. *Proteins* 2005;58:538–546.
12. Soberón X, Fuentes-Gallego P, Saab-Rincón G. *In vivo* fragment complementation of a  $(\beta/\alpha)_8$  barrel protein: generation of variability by recombination. *FEBS Lett* 2004;560:167–172.
13. Pan H, Raza AS, Smith DL. Equilibrium and kinetic folding of rabbit muscle triosephosphate isomerase by hydrogen exchange mass spectrometry. *J Mol Biol* 2004;336:1251–1263.
14. Morgan CJ, Wilkins DK, Smith LJ, Kawata Y, Dobson CM. A compact monomeric intermediate identified by NMR in the denaturation of dimeric triosephosphate isomerase. *J Mol Biol* 2000;300:11–16.
15. Nájera H, Costas M, Fernández-Velasco A. Thermodynamic characterization of yeast triosephosphate isomerase refolding: insights into the interplay between function and stability as reasons for the oligomeric nature of the enzyme. *Biochem J* 2003;370:785–792.
16. Silverman JA, Harbury PB. The equilibrium unfolding pathway of a  $(\beta/\alpha)_8$  barrel. *J Mol Biol* 2002;324:1031–1040.
17. Kannan N, Selvaraj S, Gromiha MM, Vishveshwara S. Clusters in a  $\alpha/\beta$  barrel proteins: implications for protein structure, function, and folding: a graph theoretical approach. *Proteins* 2001;43:103–112.
18. Gromiha MM, Pujadas G, Magyar C, Selvaraj S, Simon I. Locating the stabilizing residues in  $(\alpha/\beta)_8$  barrel proteins based on hydrophobicity, long-range interactions, and sequence conservation. *Proteins* 2004;55:316–329.
19. Wierenga RK, Noble MEM, Davenport RC. Comparison of the refined crystal structures of liganded and unliganded chicken, yeast and trypanosomal triosephosphate isomerase. *J Mol Biol* 1992; 224:1115–1126.
20. Maes D, Zeelen JP, Thanki N, Beaucamp N, Alvarez M, Thi MHD, Backman J, Martial JA, Wyns L, Jaenike R, Wierenga RK. The crystal structure of triosephosphate isomerase (TIM) from *Thermotoga maritima*: a comparative thermo stability structural analysis of ten different TIM structures. *Proteins* 1999;37:441–453.
21. Kursula I, Partanen S, Lambeir AM, Wierenga RK. The importance of the conserved Arg191-Asp227 salt bridge of triosephosphate isomerase for folding, stability, and catalysis. *FEBS Lett* 2002; 518:39–42.
22. Benítez-Cardoza CG, Rojo-Domínguez A, Hernández-Arana A. Temperature-induced denaturation and renaturation of triosephosphate isomerase from *Saccharomyces cerevisiae*: evidence of dimerization coupled to refolding of the thermally unfolded protein. *Biochemistry* 2001;40:9049–9058.
23. Sambrook J, Russell DW. *Molecular cloning: a laboratory manual*, 3rd ed. New York: Cold Spring Harbor Laboratory Press; 2001.
24. Vázquez-Contreras E, Zubillaga RA, Mendoza-Hernández G, Costas M, Fernández-Velasco DA. Equilibrium unfolding of yeast triosephosphate isomerase: a monomeric intermediate in guanidine-HCl and two-state behavior in urea. *Protein Pept Lett* 2000;7:57–64.
25. Norton IL, Hartman FC. Haloacetyl phosphates. A comparative study of the active sites of yeast and muscle triosephosphate isomerase. *Biochemistry* 1972;11:4435–4441.
26. Rozacky EE, Sawyer TH, Barton RA, Gracy RW. Studies of human triosephosphate isomerase: isolation and properties of the enzyme from erythrocytes. *Arch Biochem Biophys* 1971;146:312–320.
27. González-Mondragón E, Zubillaga RA, Saavedra E, Cháñez-Cárdenas ME, Pérez-Montfort R, Hernández-Arana A. Conserved cysteine 126 in triosephosphate isomerase is required not for enzymatic activity but for proper folding and stability. *Biochemistry* 2004;43:3255–3263.
28. Huang LT, Gromiha MM, Ho SY. iPTREE-STAB: interpretable decision tree based method for predicting protein stability changes upon mutations. *Bioinformatics* 2007;23:1292–1293.
29. Lambeir AM, Opperdoes FR, Wierenga RK. Kinetic properties of triosephosphate isomerase from *Trypanosoma brucei*. A comparison with the rabbit, muscle and yeast enzymes. *Eur J Biochem* 1987; 168:69–74.
30. Kursula I, Wierenga RK. Crystal structure of triosephosphate isomerase complexed with 2-phosphoglycolate at 0.83-Å resolution. *J Biol Chem* 2003;278:9544–9551.
31. Murphy KP, Freire E. Thermodynamics of structural stability and cooperative folding behavior in proteins. *Adv Protein Chem* 1992; 43:313–361.
32. Schmid FX. Kinetics of unfolding and refolding of single-domain proteins. In: Creighton TE, editor. *Protein folding*. New York: W. H. Freeman; 1992. pp 197–241.